

DOI: 10.37614/2588-0039.2020.43.002

DETECTING NEAR-TAIL CURRENT SHEET FORMATION USING ISOTROPIC BOUNDARIES: LESSONS FROM GLOBAL MHD

E.I. Gordeev and S.V. Apatenkov
Saint Petersburg State University

Abstract

A number of recent studies suggests an existence of magnetotail current sheet configurations with tailward Bz gradient during the growth phase of the substorm. Such configurations are especially interesting since they are potentially unstable for different types of instabilities and can lead to explosive reconfiguration of the magnetosphere. However, the observations are rare and ability to observe tailward gradients is very limited. Here we use the global MHD configuration with near-tail Bz minimum to investigate the regions with adiabatic and non-adiabatic behavior of energetic particles. Thus we estimate the locations of the isotropic boundaries for the modelled POES-type spacecraft flybys. We expect that the lessons learned from global MHD simulation may become helpful in exploration of non-monotonic tail current sheet configuration using observations on low-orbiting spacecraft.

1. Introduction

Magnetic fluxes in the magnetotail are largely redistributed during the substorm growth phase (GP), preparing the magnetosphere to explosive substorm activity. Recent development of the growth phase concept revealed an exceptional role of azimuthal convection in redistribution of magnetic fluxes in the near and middle magnetotail [Hsieh and Otto 2014; Gordeev et al., 2017b]. An interesting feature of the new concept is the ability to intensify the near-Earth portion of the magnetotail current sheet (CS), due to interplay between azimuthal and earthward convection intensities determined by solar wind conditions and current magnetospheric configuration. The radially localized CS intensification may lead to magnetic configuration with tailward Bz gradient, $\text{dBz}/\text{dr} > 0$, which is potentially unstable to different types of plasma instabilities, including ballooning/interchange, flapping or tearing modes [e.g. review by Sitnov et al., 2019].

The rare observational works confirm the existence of magnetotail configurations with tailward Bz gradient during GP for some events [Petrukovich et al., 2013; Ohtani and Motoba, 2017]. Recently Sergeev et al. (2018) in the case study showed the possibility to observe local B minimum during a GP, using isotropic boundaries (IB) for precipitating electrons measured on the low-orbiting POES satellites. This method gives a great opportunity for observation and qualitative interpretation of this rare magnetotail configuration. However, its validation by simultaneous measurements in the magnetotail remains difficult due to obvious lack of spacecraft coverage, but can be supported by numerical models.

Among other approaches for numerical magnetospheric modelling, the global magnetohydrodynamic (GMHD) models have several advantages important for our purpose, including: 1) they are global, which means that simulated magnetosphere is entirely embedded into the ambient solar wind and simulation do not need any special boundary conditions and predetermined configurations, providing a self-consistent modeling results; 2) simulated global MHD magnetosphere thoroughly validated and shows good agreement in the large-scale structure and dynamics for wide range of solar wind conditions [e.g., Gordeev et al., 2015, 2017a; Merkin et al., 2019]; 3) global MHD models are capable to reproduce the local near-Earth B minimum during the GP of substorms [Sergeev et al., 2018; Sorathia et al., 2020].

In this paper we present the quantitative estimation of the expected IB locations for magnetotail configuration with local B minimum, based on global MHD results.

2. MHD simulation setup

Using a set of 19 simulations, covering a wide range of solar wind parameters, Gordeev et al. (2017) investigated the global magnetic flux transport in simulated magnetospheres during loading-unloading substorm cycle. They found that the LFM GMHD model [Lyon et al., 2004] demonstrates good agreement of simulated global dynamical parameters, such as GP duration and amount of magnetic flux loading into the tail lobes, with available statistical observations. Here we use the results of two simulations from their set (Run08 and Run11) to demonstrate the development of two different types of magnetotail current sheet (CS) during the GP of substorm. Both runs have synthetic solar wind input with alternating interplanetary magnetic field (IMF) orientation periods - first two hours under northward IMF ($B_z = +6\text{nT}$ for Run08, and $+3\text{nT}$ for Run11) to supply the magnetotail plasma sheet, and last two hours under southward IMF ($B_z = -5\text{nT}$ for both) to simulate the substorm loading-unloading cycle. All other input parameters were set unchanged for Run08: IMF (B_x, B_y) = (0,4), $V_x = -600\text{ km/s}$, $N = 4\text{ cm}^{-3}$, $T = 2.5 \cdot 10^5\text{ K}$, and for Run11: IMF (B_x, B_y) = (0,4), $V_x = -400\text{ km/s}$, $N = 4\text{ cm}^{-3}$, $T = 1 \cdot 10^5\text{ K}$. Finally, we have two LFM runs,

one of them (Run11) has a typical radial profile with monotonic B_z decrease (Fig. 1a), and the second (Run08) has well developed near-Earth portion of current sheet with local B_z minimum (Fig. 1b).

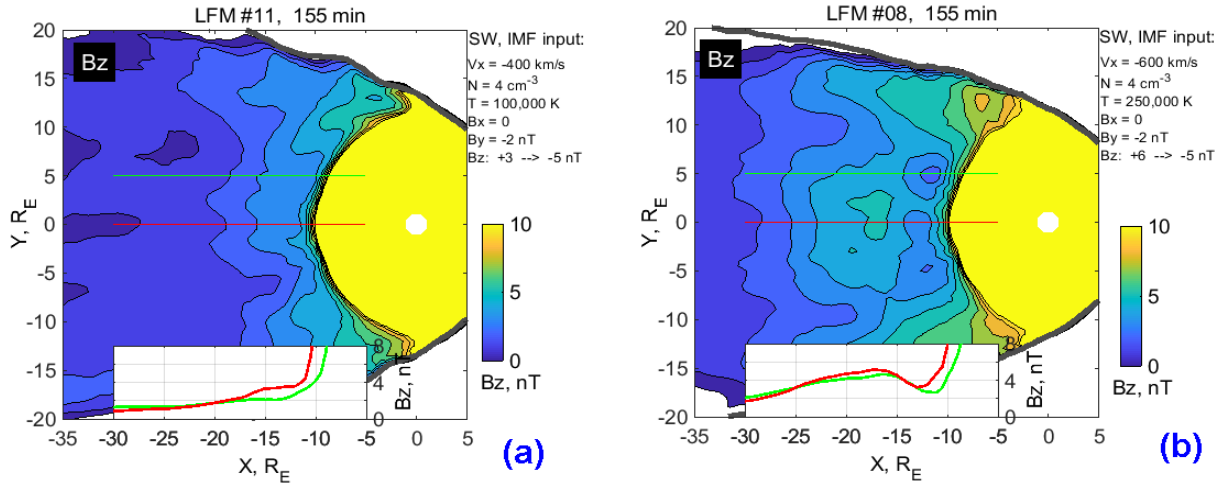


Figure 1. Distribution of B_z in the magnetospheric equatorial plane for two simulations, Run11 (a) and Run08 (b). The white plates at the bottom of each figure show the tail-aligned equatorial B_z profiles at $Y=0$ (red) and $Y=5 R_E$ (blue).

3. Expected IB locations

We assume the scattering at the field line curvature as the main mechanism for IB formation. As the condition to significant scattering and filling a loss cone we use ratio $Rc/\rho \leq K_{\text{CRIT}}$, where Rc is the field line curvature radius, ρ is a gyroradius of a particle with a given energy. Based on previous studies [Sergeev & Tsyganenko, 1982; Delcourt *et al.*, 1996] we estimate K_{CRIT} as 8. The advantage of global MHD is the ability to trace any field line and numerically estimate gradients including Rc mentioned above.

The future plan is to investigate the magnetospheric configuration properties using real IB observations with POES-like spacecraft. So we model virtual POES flybys along the constant longitude. We trace the field lines starting from the ionosphere, the start points located at the particular longitude with 0.25 degree latitudinal step. At every field line we find the point with minimal curvature radius (R_{CNS}) and minimal magnetic field magnitude (B_{NS}), neutral sheet point (NS point), this is the point to estimate Rc/ρ for different particles and check $Rc/\rho \leq K_{\text{CRIT}}$ ratio.

Further we rewrite this ratio as $B_{\text{NS}}*R_{\text{CNS}} = G*K_{\text{CRIT}}$, where $G = \sqrt{2Em}/e$ is particle rigidity, E is the particle energy, m is particle mass, e - electron charge.

We consider protons and electrons with energies corresponding to MEPED instrument onboard POES and METOP spacecraft. These are the ranges 30-80 keV, 80-240 keV, 240-800 keV for the first protons channels named P1, P2, P3; the channels E1, E2, E3 detect electrons with energies over 30 keV, 100 keV and 300 keV.

To demonstrate information simultaneously for different energy channels (with different ρ) we plot the behavior of $B_{\text{NS}}*R_{\text{CNS}}$ versus latitude and versus radial distance in the magnetosphere. Figure 2 (a, c) shows these profiles for Run11 and Figure 2 (b, d) for Run08 correspondingly. Three profiles at every panel correspond to different magnetic local times, midnight, 23h and 01h MLT. Obviously, $B_{\text{NS}}*R_{\text{CNS}}$ parameter is large close to Earth in the strong dipole field and decreases toward magnetotail with its weaker field and more curved lines. We compare $B_{\text{NS}}*R_{\text{CNS}}$ with $G*K_{\text{CRIT}}$ for every energy channel; six energy channels are shown by horizontal red dashed lines. The regions, where $B_{\text{NS}}*R_{\text{CNS}}$ is above $G*K_{\text{CRIT}}$ line, are adiabatic. The points below $G*K_{\text{CRIT}}$ are in scattering regions. The crossing points are IBs.

The profiles for “regular CS” in Figure 2 (a, c) show mostly monotonic behavior meaning the IB for every channel is unique. We also note that all six IBs are observed within a very narrow latitudinal range, less than one degree. It resembles the so-called “magnetic wall” [Sergeev *et al.*, 2015], the configuration with a very steep transition from tail-like to dipole magnetic field. Nevertheless, Figure 2c shows that the equatorial locations of six IBs cover 3-5 R_E distance range.

The decrease of the green line (23h MLT) in Figure 2 (a, c) is not monotonic. This effect is more pronounced at all profiles in Figure 2 (b, d) for Run08 with “Local minimum CS”. In the electron channels, mostly in E2 and E3, we expect to observe several IBs during a single flyby. The region in between the IBs may be referred to the local thin CS with small B_z shown in MHD simulations. The following adiabatic “island” is a product of B_z hump, the region of enhanced B_z .

The main features expected in real observations are: (1) “thin CS valley” is wider for particles with higher rigidity, (2) “adiabatic island” is wider for the particles with lower rigidity, (3) these features with secondary IBs are seen only in electron channels but not in protons. Global MHD predicts different configurations even in close local time sectors, so the IB locations can differ as well. The temporal behavior during the growth phase includes the equatorward motion of all IBs. Non-adiabatic scattering in near-tail CS may be observed during the last 20 minutes of about a 30 minute long growth phase.

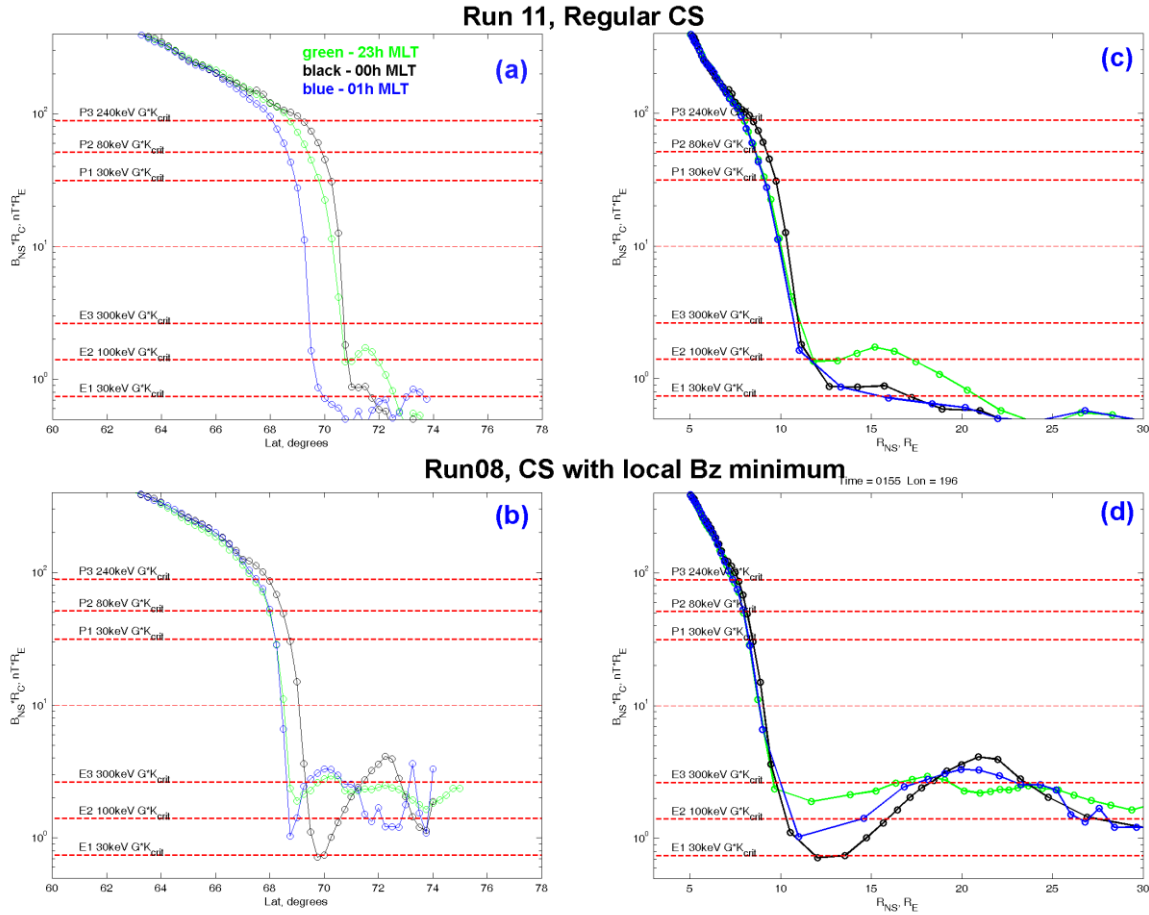


Figure 2. The profiles of $B_{NS} \cdot R_{CS}$ parameter as a dependence on latitude (a-b) and equatorial distance (c-d). The profiles are shown for two MHD simulations, Run11 and Run08. Dashed red lines depict the $G \cdot K_{CRIT}$ parameter for the particular energy channels.

4. Summary and discussion

We use global MHD modelling results to investigate the configuration of isotropic boundaries during the formation of near-tail CS with tailward B_z gradient. Findings of this numerical experiment give some insights on how to interpret the results of spacecraft measurements in future studies. In particular, the non-monotonic radial configuration of CS may be reflected in precipitating particles and their isotropic boundaries (we will refer to 30-300keV electrons) with a number of characteristics:

- 1) The near-tail portion of intense CS extends radially for ~ 5 RE, occupying $R = 10-15$ RE distances, may project to low altitude polar orbit as an electron flux isotropization in relatively narrow latitude range $\Delta LAT = 0.2-0.8^\circ$;
- 2) The portion of current sheet with enhanced magnetic field (B_z hump) occupy ~ 10 RE in radial distance, $R = 16-26$ RE, that corresponds to a significant latitudinal size of anisotropic electron flux $\Delta LAT = 2.5^\circ$;
- 3) The latitude (ΔLAT) extension of isotropic flux associated with intense near-Earth CS and anisotropic flux associated with midtail B_z hump may vary significantly depending on electron energy: ΔLAT increase for near-Earth CS and decrease for midtail B_z hump with increasing energy in channels from E1 to E3.

Acknowledgements. This work was supported by Russian Fund for Basic Research (RFBR) according to the research project 19-05-00257.

References

- Delcourt D.C., Sauvaud J.-A., Martin R.F.Jr., and Moore T.E. (1996). On the nonadiabatic precipitation of ions from the near-Earth plasma sheet. *Journal of Geophysical Research*, 101(A8), 17409–17418. <https://doi.org/10.1029/96JA01006>
- Gordeev E., Sergeev V., Honkonen I., Kuznetsova M., Rastatter L., Palmroth M., Janhunen P., Tóth G., Lyon J., and Wiltberger M. (2015). Assessing the performance of community-available global MHD models using key system parameters and empirical relationships. *Space Weather*, 13, 868–884, doi:10.1002/2015SW001307
- Gordeev E., Sergeev V., Tsyganenko N., Kuznetsova M., Rastätter L., Raeder J., Tóth G., Lyon J., Merkin V., and Wiltberger M. (2017a). The substorm cycle as reproduced by global MHD models. *Space Weather*, 15, 131–149, doi:10.1002/2016SW001495
- Gordeev E., Sergeev V., Merkin V., and Kuznetsova M. (2017b). On the origin of plasma sheet reconfiguration during the substorm growth phase. *Geophysical Research Letters*, 44, 8696–8702. <https://doi.org/10.1002/2017GL074539>
- Hsieh M.-S. and Otto A. (2014). The influence of magnetic flux depletion on the magnetotail and auroral morphology during the substorm growth phase. *J. Geophys. Res. Space Physics*, 119, 3430–3443, doi:10.1002/2013JA019459
- Lyon J.G., Fedder J.A., and Mobarri C.M. (2004). The Lyon–Fedder–Mobarri (LFM) global MHD magnetospheric simulation code. *Journal of Atmospheric and Solar-Terrestrial Physics*, 66(15-16), 1333–1350.
- Merkin V.G., Panov E.V., Sorathia K.A., and Ukhorskiy A. (2019). Contribution of bursty bulk flows to the global dipolarization of the magnetotail during an isolated substorm. *Journal of Geophysical Research: Space Physics*, 124, 8647–8668. <https://doi.org/10.1029/2019JA026872>
- Ohtani S. and Motoba T. (2017). Equatorial magnetic field of the near-Earth magnetotail. *Journal of Geophysical Research: Space Physics*, 122, 8462–8478. <https://doi.org/10.1002/2017JA024115>
- Petrukovich A.A., Artemyev A.V., Nakamura R., Panov E.V., and Baumjohann W. (2013). Cluster observations of dBz/dx during growth phase magnetotail stretching intervals. *Journal of Geophysical Research: Space Physics*, 118, 5720–5730. <https://doi.org/10.1002/jgra.50550>
- Sergeev V.A. and Tsyganenko N.A. (1982). Energetic particle losses and trapping boundaries as deduced from calculations with a realistic magnetic field model. *Planetary and Space Science*, 30(10), 999–1006. [https://doi.org/10.1016/0032-0633\(82\)90149-0](https://doi.org/10.1016/0032-0633(82)90149-0)
- Sergeev V.A., Chernyaeva S.A., Apatenkov S.V., Ganushkina N.Y., and Dubyagin S.V. (2015). Energy–latitude dispersion patterns near the isotropy boundaries of energetic protons. *Ann. Geophys.*, 33, 1059–1070, doi:10.5194/angeo-33-1059-2015
- Sergeev V.A., Gordeev E.I., Merkin V.G., and Sitnov M.I. (2018). Does a local B-minimum appear in the tail current sheet during a substorm growth phase? *Geophysical Research Letters*, 45, 2566–2573. <https://doi.org/10.1002/2018GL077183>
- Sitnov M., Birn J., Ferdousi B., Gordeev E., Khotyaintsev Y., Merkin V., et al. (2019). Explosive magnetotail activity. *Space science reviews*, 215(4), 31.
- Sorathia K.A., Merkin V.G., Panov E.V., Zhang B., Lyon J.G., Garretson J., et al. (2020). Ballooning-interchange instability in the near-Earth plasma sheet and auroral beads: Global magnetospheric modeling at the limit of the MHD approximation. *Geophysical Research Letters*, 47, e2020GL088227. <https://doi.org/10.1029/2020GL088227>